JGR Oceans

RESEARCH ARTICLE
10.1029/2021JC017552

Seasonal Hydrography of Ameralik: A Southwest Greenland Fjord Impacted by a Land-Terminating Glacier

A. E. Stuart-Lee[1], J. Mortensen[2], A.-S. van der Kaaden[1], and L. Meire[1,2]

[1]Department of Estuarine and Delta Systems, Royal Netherlands Institute for Sea Research, Yerseke, The Netherlands, [2]Greenland Climate Research Centre, Greenland Institute of Natural Resources, Nuuk, Greenland

Key Points:

- We present seasonal hydrography from a fjord system (Ameralik) in southwest Greenland impacted by a land-terminating glacier
- We compare our observations with the neighbouring Godthåbsfjord, which receives meltwater from both land- and marine-terminating glaciers
- A large fraction of the seasonal freshwater input is retained in the fjord in summer and autumn, and is exported primarily in winter

Supporting Information:

Supporting Information may be found in the online version of this article.

Correspondence to:

A. E. Stuart-Lee,
alice.stuart-lee@nioz.nl

Citation:

Stuart-Lee, A. E., Mortensen, J., van der Kaaden, A.-S., & Meire, L. (2021). Seasonal hydrography of Ameralik: A southwest Greenland fjord impacted by a land-terminating glacier. *Journal of Geophysical Research: Oceans*, *126*, e2021JC017552. https://doi.org/10.1029/2021JC017552

Received 6 MAY 2021
Accepted 7 NOV 2021

Abstract Greenland's coastal zone encompasses a large number of fjords, many of which are impacted by glacial meltwater runoff from land-terminating glaciers. This type of fjord has received limited research attention, yet may represent the future of other fjords currently impacted by marine-terminating glaciers that are retreating. In this study we describe the seasonal hydrography of Ameralik, a fjord on the southwest coast of Greenland impacted by a land-terminating glacier. To complement this analysis we compare our results with observations from the neighbouring Godthåbsfjord, which receives meltwater from both land- and marine-terminating glaciers. We find that the absence of subglacial discharge and glacial ice in Ameralik has a strong impact on the inner fjord density profiles and on circulation. The mean temperature of the upper 50 m layer was lower in Ameralik than Godthåbsfjord in May, but by September was 2°C higher in Ameralik. Dense coastal inflows occur in the late winter months in Ameralik, flushing the fjord and contributing to the return to a weakly stratified state. During the runoff period the surface waters are subject to estuarine circulation and wind forcing, while at intermediate depths a density gradient between the inner and outer fjord regions produces an intermediate baroclinic circulation, resulting in the exchange of water in this layer and the deepening of isopycnals. During summer a large fraction of the meltwater runoff is retained within the fjord rather than being exported. A substantial export of this summer accumulated freshwater occurs in connection with coastal inflows during winter.

Plain Language Summary Marine-terminating glaciers around Greenland are retreating, impacting the adjacent fjords with potential changes in the pathways taken by glacial meltwater. Few studies focus on fjords that receive meltwater only from land-terminating glaciers, although knowledge of these systems can help us better understand how water from melting glaciers eventually ends up in the ocean in a future warmer climate. Here we present a full year of temperature and salinity observations from one such fjord on the southwest coast of Greenland and use these measurements to describe seasonal changes in water properties and circulation patterns. We compare the results with observations from a neighbouring fjord which receives meltwater from both land- and marine-terminating glaciers. This comparison allows us to link differences observed between the fjords with the water movements associated with the type of glacier. While physical properties of the fjords, such as sill depth, play an important role in the circulation, the meltwater pathway also influences fjord hydrography, most prominently in the surface layers. This study will help us to understand the potential future state for many Greenland fjords with glaciers that are presently marine-terminating.

1. Introduction

As a consequence of rapid climate change in the Arctic region, the Greenland Ice Sheet (GrIS) has suffered substantial mass loss in recent decades (Shepherd et al., 2020; Simonsen et al., 2021; Smith et al., 2020). For the surrounding fjord systems this translates to large scale glacial retreat with increased freshwater fluxes into fjords (e.g., King et al., 2020; Rignot et al., 2016). Changes in fjord hydrography subsequently affect the range of roles performed by these systems that act as transition zones between the GrIS and the open ocean. They support complex and productive ecosystems (Arendt et al., 2016; Meire et al., 2017), play a key role in regulating heat transport to glaciers, and transform and export freshwater from the GrIS to the continental shelf (Beaird et al., 2018; Mortensen et al., 2018; Straneo & Cenedese, 2015).

A major challenge in predicting the response of fjords to glacial retreat, as well as other consequences of climate change, lies in the inherent diversity of these systems. Hydrography in fjords is not easily generalized, owing in part to the contributions of regional differences (e.g., ocean water masses, local climate) and variation in physical

features (e.g., fjord bathymetry, freshwater sources, tides). This drives the need for studies into a range of fjords across Greenland. Changes in marine-terminating glaciers are responsible for most of Greenland's contribution to sea level rise in recent decades (King et al., 2020; Mouginot et al., 2019). The fjords in which these glaciers terminate have received considerable research attention, with particular focus on subglacial discharge and its related upwelling mechanism which contributes to the unique hydrography of these fjords (e.g., Mankoff et al., 2016; Mortensen et al., 2020; Sciascia et al., 2013; Straneo et al., 2011).

Although fjords impacted by land-terminating glaciers represent a substantial remaining proportion of Greenland's coast and key export routes for meltwater from the Greenland Ice Sheet to the ocean, few studies focus on this type of fjord (e.g., Dmitrenko et al., 2015; Nielsen et al., 2010). One such example is Kangerlussuaq, a fjord on the west coast (66.8°N, 51.5°W), which only receives glacial meltwater via river runoff. The inner part of Kangerlussuaq is segregated from the ocean by a 100 km long shallow outer section, almost decoupling the inner fjord from coastal dynamics. As such, fjord hydrography is strongly determined by meltwater runoff in summer, driving stratification and estuarine circulation, and by sea ice formation in winter, forming dense water through brine release (Lund-Hansen et al., 2018; Monteban et al., 2020; Nielsen et al., 2010).

In addition, research has been carried out in the Young Sound/Tyrolerfjord system on the northeast coast (74.4°N, 20.4°W) which is also impacted only by meltwater runoff via land. Estuarine circulation resulting from this runoff characterises this system in summer, while polynyas and tide-driven fjord-shelf exchange are drivers of a two-layer circulation in winter that extends up to ∼150 m depth (Bendtsen et al., 2014; Boone et al., 2017; Dmitrenko et al., 2015). Young Sound has a very shallow outer sill of ∼45 m depth that is a topographic barrier to the ocean (Rysgaard et al., 2003), and its location on the east coast means that it is impacted by different coastal water masses (associated with the East Greenland Current) than those found on the west coast (Rysgaard et al., 2020). Variation observed in seasonal climate, coastal water masses and other physical differences such as bottom topography leads to a need for high resolution and seasonal studies of other fjords impacted by land-terminating glaciers.

Here we describe for the first time the seasonal hydrography, inferred circulation patterns and meteorological conditions of Ameralik, a fjord impacted by a land-terminating glacier, which is located next to Godthåbsfjord on the southwest coast of Greenland (Figure 1a). Transects from March–December 2019 and observations from March 2020 provide a unique description of changing seasonal conditions in Ameralik. We compare our data to observations from Godthåbsfjord, which, in contrast to Ameralik, is impacted by three marine-terminating glaciers in addition to three land-terminating glaciers. The seasonal hydrography of Godthåbsfjord has been described extensively (Mortensen et al., 2011, 2013, 2014, 2018), providing a breadth of existing knowledge including a baseline study on the surrounding water masses to aid the analysis of Ameralik. Additionally, hydrographic surveys conducted in 2019 allow a closer comparison. We investigate the roles of land- and marine-terminating glaciers in order to highlight fundamental differences between the two systems and contribute toward our understanding of potential future fjord transitions under glacial retreat.

2. Study Area and Methodology

2.1. Regional Setting

Ameralik is located on the southwest coast of Greenland close to Nuuk (Figure 1a). The fjord is ∼75 km long, 5–7 km wide and has an area of ∼400 km^2. A ∼110 m deep sill is found at the entrance to the fjord and the central part is characterized by a sequence of deep basins reaching a maximum depth of ∼700 m (Figure 1b). The tidal range for Nuuk is ∼1–5 m (Richter et al., 2011). The fjord remains largely ice-free throughout the year, with sea ice only found close to the river delta in the inner part of the fjord during winter. No glaciers terminate directly in the fjord, though glacial meltwater is delivered via runoff from rivers. Meltwater is primarily supplied by the glacial river Naajat Kuuat (Figure 1a), which drains a catchment area of ∼356 km^2 of the Greenland Ice Sheet. For 2012, discharge from the river was estimated as 0.78 km^3 yr^{-1} (Overeem et al., 2015).

Godthåbsfjord (Nuup Kangerlua) is the neighbour fjord to Ameralik on the northern side (Figure 1a). It has a length of ∼190 km and a surface area of 2,013 km^2 extending over several fjord branches and containing multiple sills. The main sill is located at the entrance with a depth of ∼200 m and the deepest point is 620 m (Mortensen et al., 2011, 2018). In Godthåbsfjord, meltwater and glacial ice are delivered by three marine-terminating glaciers and three land-terminating glaciers via rivers. Estimates from a regional climate model for freshwater input are

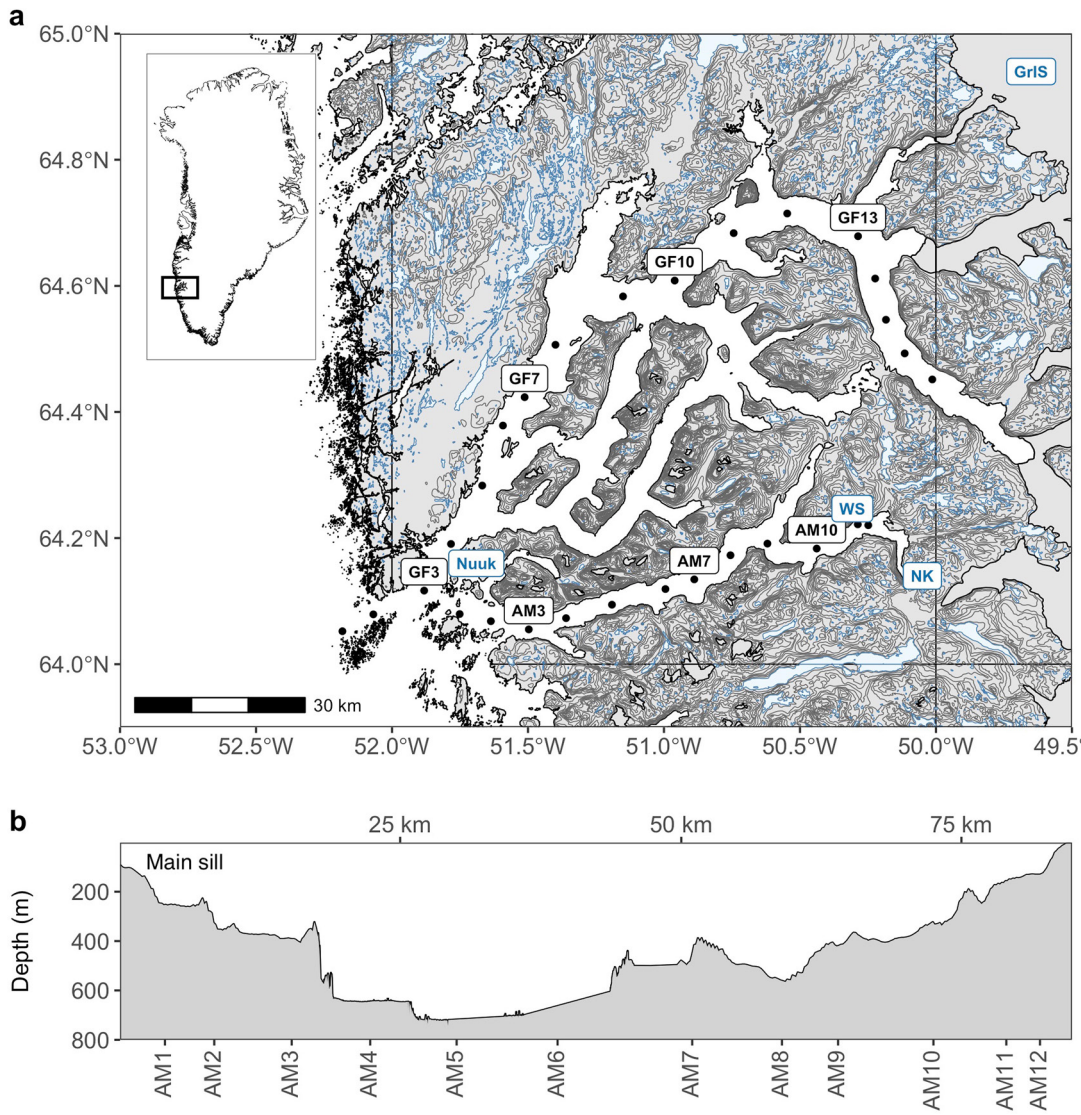

Figure 1. (a) Map of Ameralik and Godthåbsfjord. Standard CTD station locations are indicated by solid black circles. Selected stations are labeled in black (prefixed with "GF" for Godthåbsfjord or "AM" for Ameralik). Other sites are labeled in blue: Nuuk, the Greenland ice sheet ("GrIS"), the weather station in Ameralik ("WS"), and the river Naajat Kuuat ("NK"). The study area is identified on the inset map of Greenland. (b) Bathymetry section of Ameralik with approximate station positions indicated.

18.4 ± 5.8 km^3 yr^{-1} for the marine-terminating glaciers, excluding solid ice discharge, and 7.5 ± 2.1 km^3 yr^{-1} for the land-terminating glaciers (based on the period 2002 to 2012, Langen et al., 2015). Solid ice discharge from the three marine-terminating glaciers is estimated at 7–10 km^3 w.e. yr^{-1} (Van As et al., 2014). Sea ice is present seasonally in the innermost part of Godthåbsfjord (from near station GF13 inwards, Figure 1a).

The coastal waters outside of Ameralik and Godthåbsfjord are characterized by distinct water masses (winter mode waters: Rysgaard et al., 2020). The upper layer is composed of relatively cool and fresh southwest Greenland coastal water (θ-S properties ~0°C and 33) arriving from the south with an origin in the East Greenland Current and runoff from Greenland. In summer 2016 this coastal water was identified in the upper 200 m of the water column at 64°N, close to Ameralik and Godthåbsfjord (Rysgaard et al., 2020). At greater depths, warmer and more saline subpolar mode water of Atlantic origin is present, which is subdivided into upper subpolar mode water (θ-S properties ~6°C and 35) and deep subpolar mode water (θ-S properties ~4°C and 34.7) (Lin et al., 2018; Rysgaard et al., 2020). The thickness of the combined subpolar mode water layer varied between 0 and 600 m along the southwest coast of Greenland in summer 2016 (Rysgaard et al., 2020). The seasonal presence

of cold and relatively saline Baffin Bay polar water (θ-S properties ~−1.8°C and 33.6) of northern origin can occasionally be observed in a diluted form outside the fjords (Rysgaard et al., 2020).

2.2. Sampling

Air temperature, photosynthetically active radiation (PAR), wind speed and wind direction data were measured with 10 min resolution in 2019 for Ameralik using an Onset weather station located on land in the inner part of the fjord on the north side (64°13.42'N, 50°18.12'W, Figure 1a). In its vicinity a SBE microcat mooring (SBE 37-SMP, SeaBird) was fixed to the bedrock at a mean depth of ~6 m, just outside the intertidal zone, measuring the surface layer water temperature, salinity and pressure with 10 min resolution. Air temperature and wind speed were obtained from the meteorological station in Nuuk (Asiaq, Greenland Survey).

Due to practical limitations it was not possible to assess potential rotational effects in Ameralik. However, earlier work based on cross-fjord sampling in Godthåbsfjord found limited cross-fjord variation with the dominant flow being in the along-fjord direction (Mortensen et al., 2014). As Ameralik is narrower than Godthåbsfjord, cross-fjord variation is presumed to also be limited, resulting in the focus on the along-fjord gradient. Seasonal measurements were made at 12 standard stations in Ameralik spaced between 3 and 13 km from one another (AM1 to AM12 in Figure 1a) in May, July and September 2019. Longer term fjord sampling was also carried out at monthly intervals from March–December 2019 at selected stations (AM3, AM5, AM7, AM10, AM11 and AM12) and in March 2020 at station AM5.

Additionally, sampling was conducted at 13 standard stations in Godthåbsfjord (GF1 to GF13 in Figure 1a) in May, July and September 2019. Favourable ice conditions in the inner fjord during the September campaign allowed the sampling of 4 further standard stations (GF14 to GF17). Longer term fjord sampling in Godthåbsfjord was also carried out at monthly intervals from February to December 2019 at selected stations from GF5 and inwards.

At every station, depth profiles of conductivity, temperature and pressure were collected using a SeaBird SBE-19plus CTD and averaged over 1 m vertical depth intervals. Sensors were calibrated annually by the manufacturer and salinity precision was typically within the range of 0.005–0.010. Sampling took place aboard the Greenland RV Sanna and Avataq, and the commercial Greenland vessels Polar Dive and Tulu. For comparison with previous field programs, potential temperature (ITS-90) and practical salinity are used throughout the text.

Freshwater content (FWC) represents the portion of the water column composed of freshwater, expressed in meters. This was calculated for salinity profiles with 1 m resolution at depth ranges 0–50, 50–200 and 200–500 m at station AM5 according to the equation:

$$\mathrm{FWC} = \int_{z_b}^{z_a} \frac{S_{\mathrm{ref}} - S(z)}{S_{\mathrm{ref}}}\,\mathrm{dz}$$

where z is the depth, a and b are the top and bottom depths, S is the measured salinity, and S_{ref} is the reference salinity, which was set at 33.3. This value is the maximum salinity measured in Ameralik across the sampled period (at station AM5 in March 2019).

The stratification index (φ, J m^{-3}) represents the energy required to completely mix the water column (Simpson, 1981) and was calculated according to the equation of MacKenzie and Adamson (2004):

$$\varphi = \frac{1}{h-1}\int_{-h}^{0}\left(\rho - \overline{\rho}\right) g\, z\,\mathrm{dz}$$

integrating from a constant depth h to the sea surface and where ρ is the measured density at the vertical coordinate z, $\overline{\rho}$ is the mean density from the sea surface to h, and g is acceleration due to gravity (9.81 m s^{-2}). To compare differences in the surface layer, this calculation was based on density profiles from the upper 50 m for all stations except AM12, for which the upper 36 m was used (maximum depth of the station). All processing of data was done using the open-source programming language R (R Core Team, 2013).

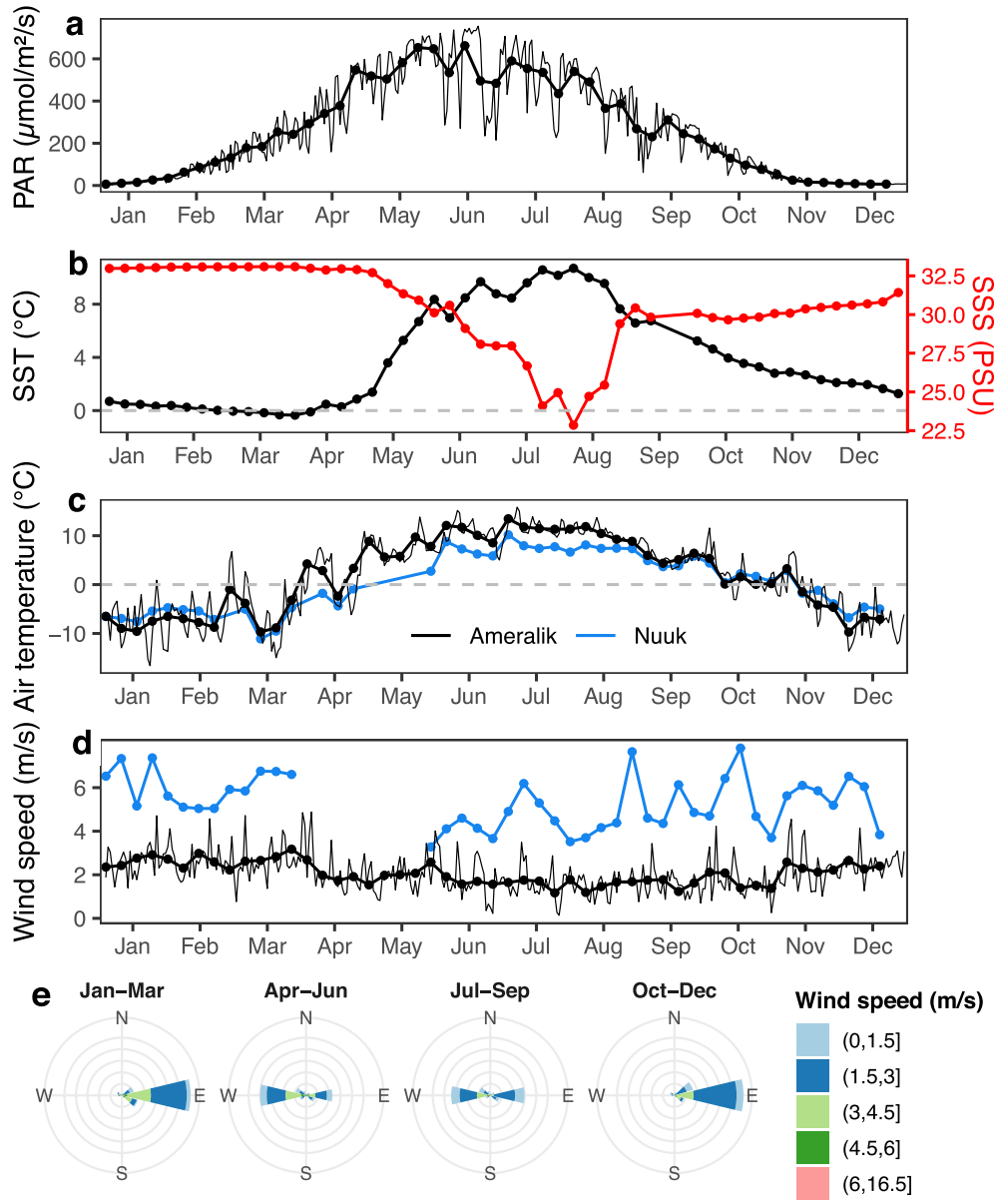

Figure 2. Weather conditions for Ameralik and Nuuk in 2019. Weekly mean values (solid circles, thick lines), and daily means (thin lines) for (a) photosynthetically active radiation at Ameralik weather station, (b) sea surface temperature (black) and sea surface salinity (red) at Ameralik mooring, (c) air temperature, and (d) wind speed at Ameralik weather station (black) and Nuuk weather station (blue). Month labels on the *x*-axes of (a–d) appear in the middle of the month. (e) Quarterly windroses for Ameralik.

3. Results

3.1. Weather Observations

Data from the weather station in the inner part of Ameralik (Figure 1a) show low incoming solar radiation in the winter of 2019, with a mean PAR of ∼16 µmol m^{-2} s^{-1} in January (Figure 2a). Air temperatures in winter reached a low of −18°C (Figure 2c). The gradual increase in incoming radiation during spring resulted in positive monthly mean temperatures starting from April and peaking in July at 12°C. Compared to similar measurements collected in Nuuk in 2019, air temperatures in the inner part of Ameralik were colder in winter and warmer in summer (Figure 2c). The mean temperature in January was −8.3°C at the Ameralik station, and −6.4°C in Nuuk,

and in June these were 10.3°C and 6.5°C respectively. This is in line with similar observations in the region showing a clear land-ocean gradient (Abermann et al., 2019).

Distinct seasonal changes were also found in the wind patterns in Ameralik, with the highest mean daily wind speeds occurring between November and April. Wind speeds further out of the fjord were generally higher, as can be seen from a comparison with Nuuk, close to the coast (Figure 2d). Throughout the year, wind was usually oriented along the fjord axis, as observed in other Arctic fjords (e.g., Svendsen et al., 2002), with the steep mountainous terrain of Ameralik contributing with orographic effects (Figures 1a and 2e). From January to March, and from October to December (roughly corresponding to winter months), winds blew predominantly out-fjord (easterly wind) throughout the day (Figure 2e). From April to September, as the land became warmer than the sea, the dominant wind direction was in-fjord (westerly wind) (Figure 2e). Transitions between these two modes took place during April and late August to September. The summer winds were less uni-directional and changes in wind direction occurred during the day due to differential heating between land and sea. Generally there was in-fjord wind during the day and weaker out-fjord wind at night.

3.2. Seasonal Hydrographic Observations in Ameralik

Owing to its mostly glacial source, freshwater runoff to the fjord is highly seasonal and increases approximately in line with air temperature once above 0°C. This corresponds to little to no runoff between October and April (Van As et al., 2014). In March 2019, air temperature remained well below 0°C, corresponding to low freshwater runoff. Under these conditions, increased wind speeds, together with tides, promoted mixing of the water column. This is reflected in a relatively uniform cold (∼0°C) and saline (∼33.1) water column with weak stratification and little horizontal or vertical variation (Figures 3a and 3b).

As air temperature and insolation rose through spring and summer, the surface water warmed and produced an along-fjord surface gradient with temperatures increasing from outer to inner fjord (Figures 3c and 3e). Mooring data demonstrate the time lag between sea surface layer temperature and insolation (Figures 2a and 2b). Sea surface layer temperature at the mooring (∼6 m depth, depending on the tide) increased quickly in May, with a rise of 7.5°C in the weekly mean. In May, a shallow thermocline started to develop in the upper 10 m, most prominently from the midfjord (AM5) to the innermost station (AM12). In this range the mean potential temperature of the upper 10 m layer was 1.9°C and the mean salinity was 32.8. At the mouth of the fjord (AM1 and AM2), vertical gradients near the surface were limited.

In subsequent months, increased freshwater runoff further strengthened the surface stratification through the establishment of a thin layer of relatively fresh (mean salinity <31) water in the upper 10 m of the central and inner fjord stations (AM5 to AM12). Driven by the estuarine circulation, which results in a net out-fjord flow in the surface layer, the freshwater runoff originating in the inner fjord was transported out-fjord. By July, following high levels of freshwater runoff, this surface layer was well defined along Ameralik with salinity as low as 6 in the inner part of the fjord (station AM12) and a strong halocline in the upper 6 m of the central and inner fjord stations (AM5 to AM12, Figures 3e and 3f). The upper 10 m layer of this range had a mean potential temperature of 8.0 °C and mean salinity of 28.6. The intermediate depths (50–200 m) freshened and warmed during this period (Figures 3c–3f, 4a and 4b), which we explain in Section 4.1.

As September arrived, the air temperatures dropped below those of the surface waters (Figures 2b and 2c) and freshwater input will have declined strongly (Van As et al., 2014), leading to higher salinity in the surface layer and a less pronounced halocline. Together with increased winter storms (evidenced by higher daily mean gust speeds in the winter months, Figure S1), this resulted in a much weaker surface stratification throughout the fjord by the end of the year (Figures 3i and 3j). The upper 10 m layer from station AM5 to AM12 had a mean potential temperature of 6.3°C and mean salinity of 30.2 by September. At intermediate depths (50–200 m) we observe a gradual deepening of isopycnals during autumn (September–November, Figures 3g–3j), determined primarily by the changes in salinity (dashed line representing the 200 m depth in Figures 4b and 4c).

3.3. Retention of Summer Accumulated Freshwater in Ameralik

To assess changes in freshwater, freshwater content (FWC) was calculated for a station in the central fjord (AM5) using the maximum salinity in Ameralik in March 2020 as the reference value. A significant freshening took

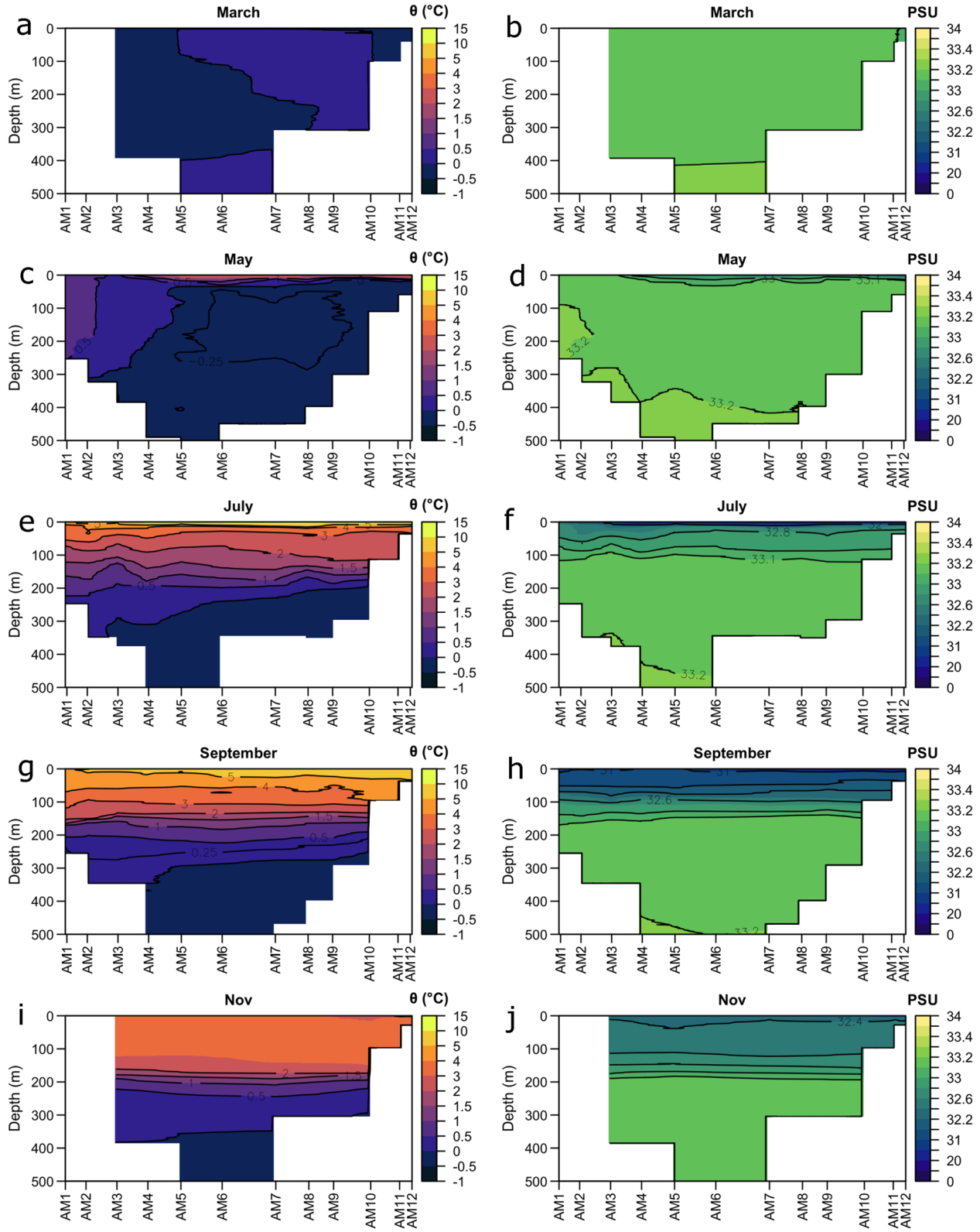

Figure 3. Bimonthly potential temperature and practical salinity length sections of upper 500 m of Ameralik from March to November 2019, from outer fjord (left) to inner fjord (right). March and November data are from long term Ameralik monitoring; May to September data are from the seasonal campaigns with higher horizontal spatial resolution.

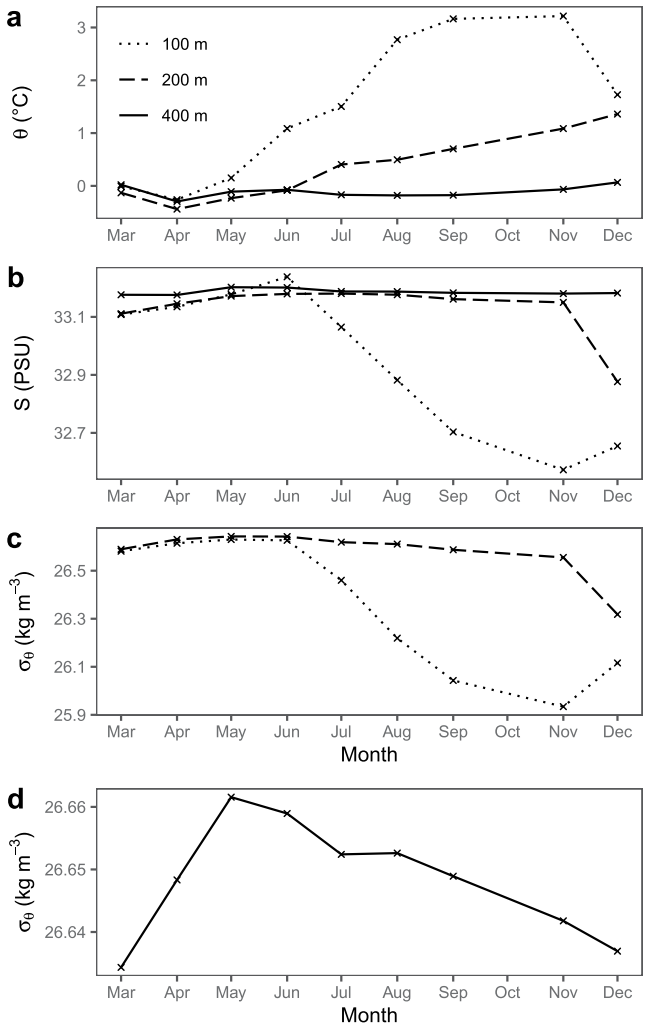

Figure 4. Time series of water properties at station AM5 in 2019: (a) potential temperature at 100, 200 and 400 m, (b) practical salinity at 100, 200 and 400 m, (c) potential density anomaly at 100 and 200 m, and (d) potential density anomaly at 400 m. Line types represent depths: dotted for 100 m, dashed for 200 m, and solid for 400 m. Note the difference scales used in (c) and (d) for potential density anomaly.

place at station AM5 between June and August, with an increase in FWC of the upper 500 m layer of 4.4 m (Figure 5). This was followed by a decrease of 1.2 m between August and December. Considering individual layers during this period of decline in the second half of the year, the surface layer (0–50 m) FWC decreased by 2.1 m, while that of the intermediate layer (50–200 m) increased by 0.7 m, and that of the deep layer (200–500 m) increased by 0.3 m. This shows that a large fraction of the freshwater discharged during the summer months remained within the fjord rather than being directly exported.

3.4. Winter Fjord Water Renewal in Ameralik

The deep water (below 400 m) is fairly isolated owing to the combination of a shallow entrance sill (~110 m) and deep basin (Figure 1b). As such, this water is decoupled from the seasonal changes observed in the upper water column and its properties remained stable for much of 2019 (Figure 4). Due to diffusion processes the density of the basin water gradually lowers (Figure 4d), reducing the density difference between the coastal water and the fjord. In this way, the basin water becomes preconditioned for dense coastal inflows, whereby coastal water enters over the sill and replaces the resident fjord water. Mid-fjord measurements are not available for January and February 2019, but we identify dense coastal inflow in late winter/early spring 2019 from the increase in potential density anomaly of 0.03 kg m^{-3} at 400 m between March and May (Figure 4d) and associated increase in salinity of 0.26 (Figure 4b). This increase cannot be attributed to the process of brine rejection due to the lack of sea ice and drifting sea ice in Ameralik during winter. Nor can wind forcing or convection be the primary cause as this would result in decreased salinity. Winter dense coastal inflow has also been observed in the neighbouring Godthåbsfjord (Mortensen et al., 2018). Following this period of deep water renewal in Ameralik, the density of the basin water was at its highest, and further dense coastal inflow events are not observed during the summer months.

There was a substantial decrease of 1.9 m in FWC between December 2019 and March 2020 (Figure 5), which may be representative of an annual pattern, i.e., a large freshwater export occurring each winter. If this is the case, the period can be characterized by a flushing of the summer accumulated freshwater throughout the fjord. From the approximated surface area of ~400 km^2 and the difference of 1.9 m in FWC at AM5 between December 2019 and March 2020, we estimate an export of ~0.8 km^3. This is very close to the estimated annual river discharge of 0.78 km^3 reported in Section 2.1. The estimated export is most pronounced in the intermediate layer (50–200 m), with a 1.5 m decrease between December 2019 and March 2020. We hypothesise that a fraction of the meltwater discharged to the surface layer is retained within the fjord system and only flushed out of the intermediate layer after the summer, indicating that the winter period plays an important role for the freshwater export.

3.5. Water Masses in Ameralik and Godthåbsfjord

Potential temperature and salinity (θ-S) curves from a selection of stations in Ameralik and Godthåbsfjord in July and December 2019 are shown in Figure 6. Changes in insolation and volumes of meltwater input result in a large difference in temperature and salinity ranges between summer and winter. In July, the θ-S curves show the relatively warm and fresh summer surface water from the surface layers of the inner fjords (Figure 6a). This summer surface water originated from runoff (i.e., freshwater runoff to the surface layer) and net precipitation, which was subsequently warmed by solar radiation. In Godthåbsfjord, a prominent dip in temperature and salinity identifies the body of cool and fresh subglacial water below the summer surface water in the inner part of the fjord

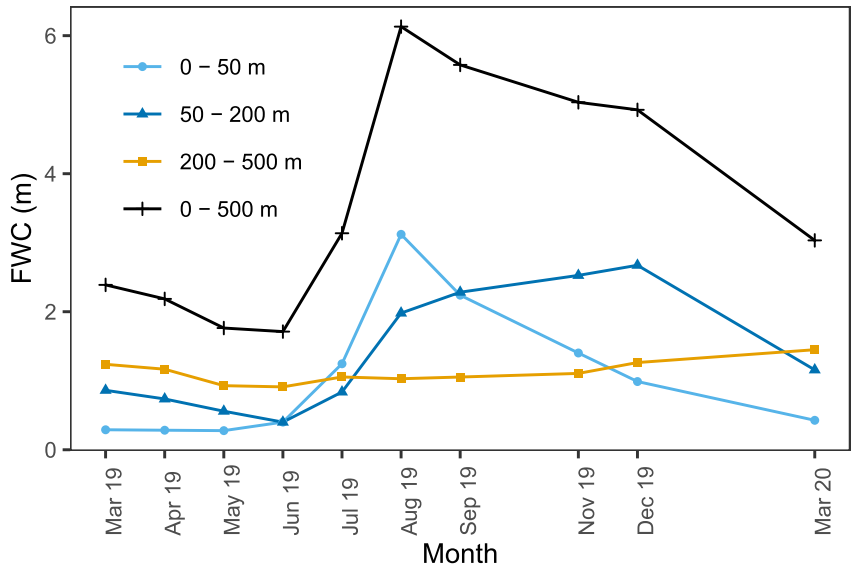

Figure 5. Monthly Freshwater Content (FWC, m) at AM5 in Ameralik from March 2019 to March 2020. Calculated with a practical salinity reference value of 33.3.

(Figure 6a). This subglacial water, which is not found in Ameralik, has its origin in the subglacial discharge of freshwater discharged at the grounding line of marine-terminating glaciers. The discharge undergoes modification by entrainment as it ascends toward the surface, and then by cooling from the ice mélange as it is transported

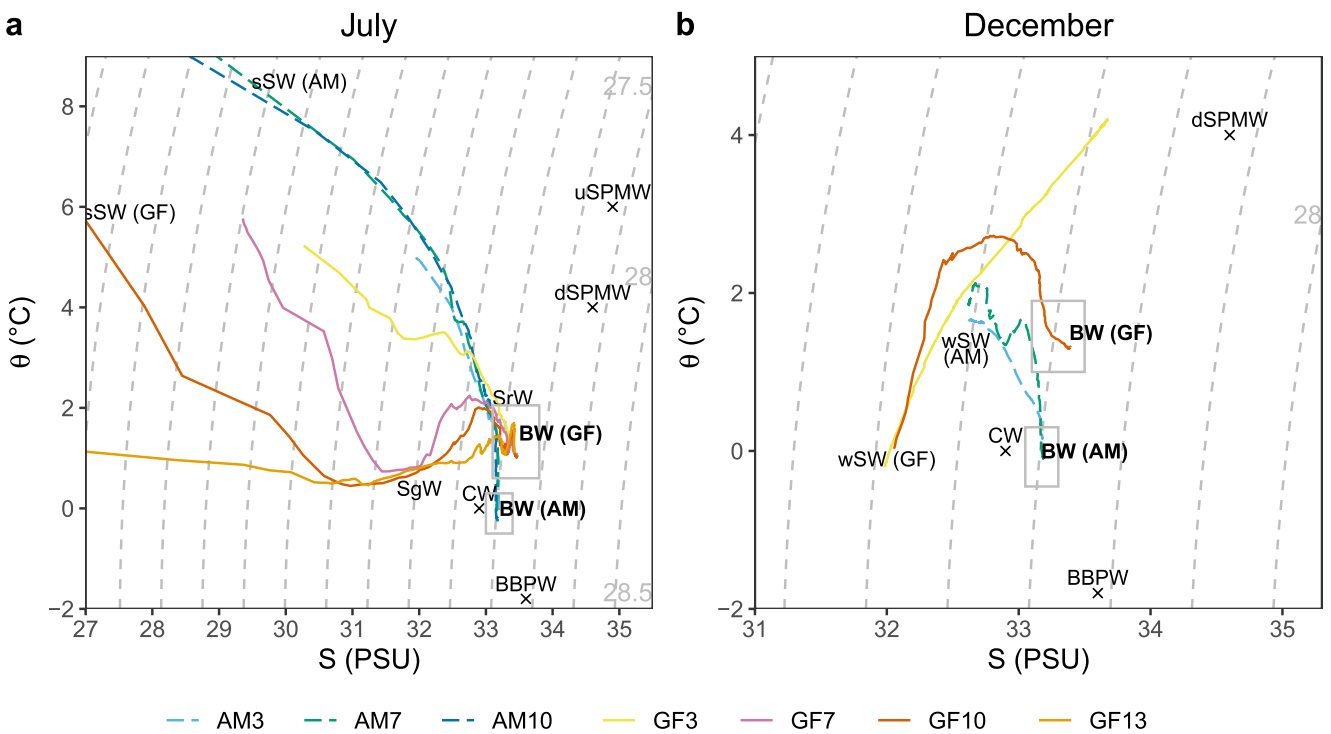

Figure 6. Potential temperature and practical salinity observations from selected stations in Ameralik (dashed lines) and Godthåbsfjord (solid lines) in (a) July, and (b) December 2019. Each line represents the depth profile from one station. The July plot is cropped to exclude observations of practical salinity below 27 and potential temperature above 9°C. Approximate positions of coastal (Rysgaard et al., 2020) and fjord (Mortensen et al., 2011) water masses are indicated with acronyms: BBPW, Baffin Bay polar water; CW, southwest Greenland coastal water; dSPMW, deep subpolar mode water; uSPMW, upper subpolar mode water; SgW, subglacial water; SrW, sill region water; sSW, summer surface water; wSW, winter surface water; BW, basin water. The gray basin water rectangles indicate water range in 2019 below 400 m. The gray dashed lines are isopycnals.

away from the glacier, and ends up below the summer surface layer (Bendtsen et al., 2015; Mankoff et al., 2016; Mortensen et al., 2020).

The layer below the subglacial water contained sill region water, an intermediate water mass which originates in the outer sill region where tidal-induced diapycnal mixing takes place between a number of near surface water masses (i.e., summer surface water, subglacial water and coastal water) (Mortensen et al., 2011). In Godthåbsfjord, sill region water can be identified by the temperature maximum relative to the cooler subglacial water layer found above (Mortensen et al., 2011). Because Ameralik does not contain subglacial water, the profiles lack the corresponding subsurface temperature minimum from which to identify the sill region water. It can however be approximated from the overlap in properties with sill region water in Godthåbsfjord (Figure 6a). The similarity of these properties suggests that this is the same water mass, and that the same mechanism is therefore involved in its formation in Ameralik as in Godthåbsfjord, which is further discussed in Section 4.1.

Below the layer containing sill region water was the relatively cool and saline basin water, identified in Figure 6 with gray boxes. This occupied the water column down to the bottom, remaining almost stagnant for most of the year with intermittent periods of renewal during winter.

In winter, cooling and reduced freshwater runoff was responsible for the formation of winter surface water and fjord properties were dominated by basin water, a fjord water mass with close connection to the coastal water masses (Figure 6b).Observations from sampled central fjord stations in March 2019 show that the mean properties of the upper 10 m layer were slightly cooler and more saline in Ameralik (−0.1°C, 33.1) than in Godthåbsfjord (0.3°C, 32.9).

3.6. Fjord Comparison of Upper Water Column Properties

The seasonal hydrography of Godthåbsfjord is well documented (Mortensen et al., 2011, 2013, 2018, 2020) and the focus here is on the comparison with Ameralik.

Figure 7 presents the mean potential temperature of the upper 50 m layer at each station through the studied months. Temperatures near the shared mouth region of the two fjords remained similar, but further in-fjord diverged considerably. In May, at the start of the melt season, the upper 50 m layer of Ameralik (mean of stations AM1 to AM12) was 0.6°C cooler than in Godthåbsfjord (mean of stations GF1 to GF13), which relates to the differences in entrance sill depth and associated basin water temperatures. As discussed below in Section 4.2, the basin water of Ameralik in 2019 was cooler than that of Godthåbsfjord. During winter flushing, a portion of the basin water was displaced upwards (e.g., Mortensen et al., 2018), consequently affecting the temperature of the upper water layers. The lower temperatures in the basin water of Ameralik and inflow of cooler water are both likely to have contributed to the colder subsurface layer compared to Godthåbsfjord. During winter and spring, icebergs in Godthåbsfjord remained mostly trapped in the innermost fjord by sea ice (i.e., in the ice mélange), which may have limited their cooling influence at that time. However, large changes in surface layer properties between the studied months show the influence of the strong meltwater input in Godthåbsfjord (composed of runoff, subglacial freshwater discharge and net precipitation) as well as the presence of large quantities of icebergs further out-fjord (observed during fjord sampling). As a result, by July the upper 50 m layer of Ameralik was warmer than the upper 50 m of Godthåbsfjord, and by September the difference in mean temperature of the upper 50 m was 2°C (Figure 7).

The extra freshwater input in Godthåbsfjord does not lead to increased overall stratification: the stratification index is higher in Ameralik than in Godthåbsfjord in the mid- and outer fjord in July (Figure 8). This can be explained by the presence of subglacial discharge in Godthåbsfjord, whereby the freshwater released at depth forms buoyant plumes that entrain surrounding ambient water, bringing deep fjord water toward the surface and mixing the water column (Bendtsen et al., 2015). The subglacial water forms an out-fjord flow below the shallow surface layer that originates from runoff (~10–30 m depth range, Figures 9c and 9e). In this way, subglacial discharge has an impact on the vertical structure of the water column throughout the fjord. Increases in runoff can have a similar effect by causing a thinning of the surface layer (Bendtsen et al., 2014). In May, the surface layer in Ameralik was shallower than in Godthåbsfjord, but by July, as freshwater input increased, this layer was shallower in Godthåbsfjord than in Ameralik (Figures 10b and 10c).

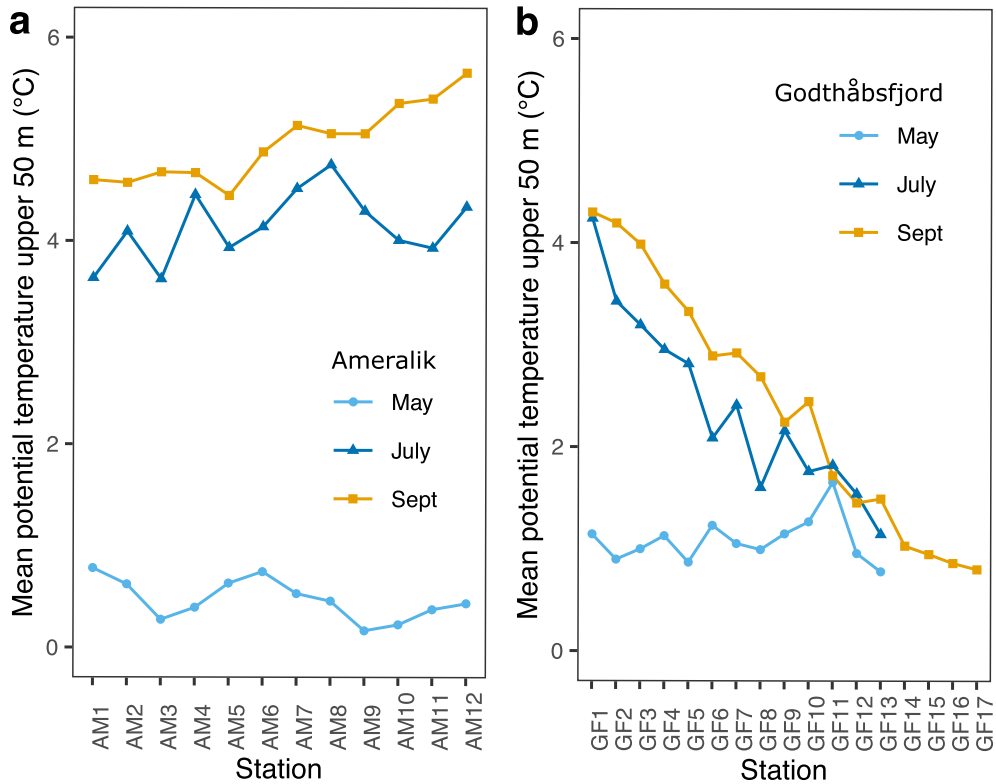

Figure 7. Mean potential temperature in the upper 50 m depth layer of each station in (a) Ameralik, and (b) Godthåbsfjord in May, July and September 2019.

4. Discussion

4.1. Fjord Circulation Comparison

By winter, seasonal change in Ameralik led to the disappearance of the summer stratification, whereas in Godthåbsfjord some stratification remained (Figure 10a). These seasonal changes are influenced by a combination of mixing mechanisms including tides and dense coastal inflows, which in Ameralik resulted in a flushing of the fjord, as has been inferred from the increasing basin water density discussed in Section 3.4. Godthåbsfjord also experiences dense coastal inflows, but in Godthåbsfjord the deep water does not completely renew (e.g., Mortensen et al., 2018). The presence of sea ice also contributes to the perseverance of stratification in Godthåbsfjord by providing a barrier to wind mixing (Meire et al., 2015). As observed in Ameralik, it may be that during the winter period (when dense coastal inflow is active) Godthåbsfjord also undergoes a large export of summer accumulated freshwater. The FWC calculations in 2008–2009 show that FWC at intermediate depths (30–277 m) dropped from 4.1 m in November to 1.5 m in May (based on a reference salinity of 33.56, Mortensen et al., 2011).

In the intermediate water layer (50–200 m) of Godthåbsfjord in July there was an inflow of a warm tongue extending from the fjord entrance (Figure 9c). From station GF5 inwards this can be observed beneath the cooled layer of subglacial water (~10–30 m) that is itself below the warmer surface layer (~0–10 m). This is referred to as intermediate baroclinic circulation by Mortensen et al. (2011) and develops with a compensation out-flow below, lowering the isopycnals in the fjord. This circulation was later supported by direct current measurements (Mortensen et al., 2014). It is present year-round in Godthåbsfjord (Figures 11b and 11d), driven by density differences between the inner and outer fjord and the shelf/coast. It is the most dominant circulation in summer when the combination of tidal mixing in the outer sill region and warming and freshening of surface fjord water results in the outer fjord water becoming less dense than the inner fjord (Mortensen et al., 2014).

We hypothesise that the intermediate baroclinic circulation is also present in Ameralik. Ameralik also displayed steady warming and freshening in its intermediate layer during summer (Figures 3e and 3f) and associated

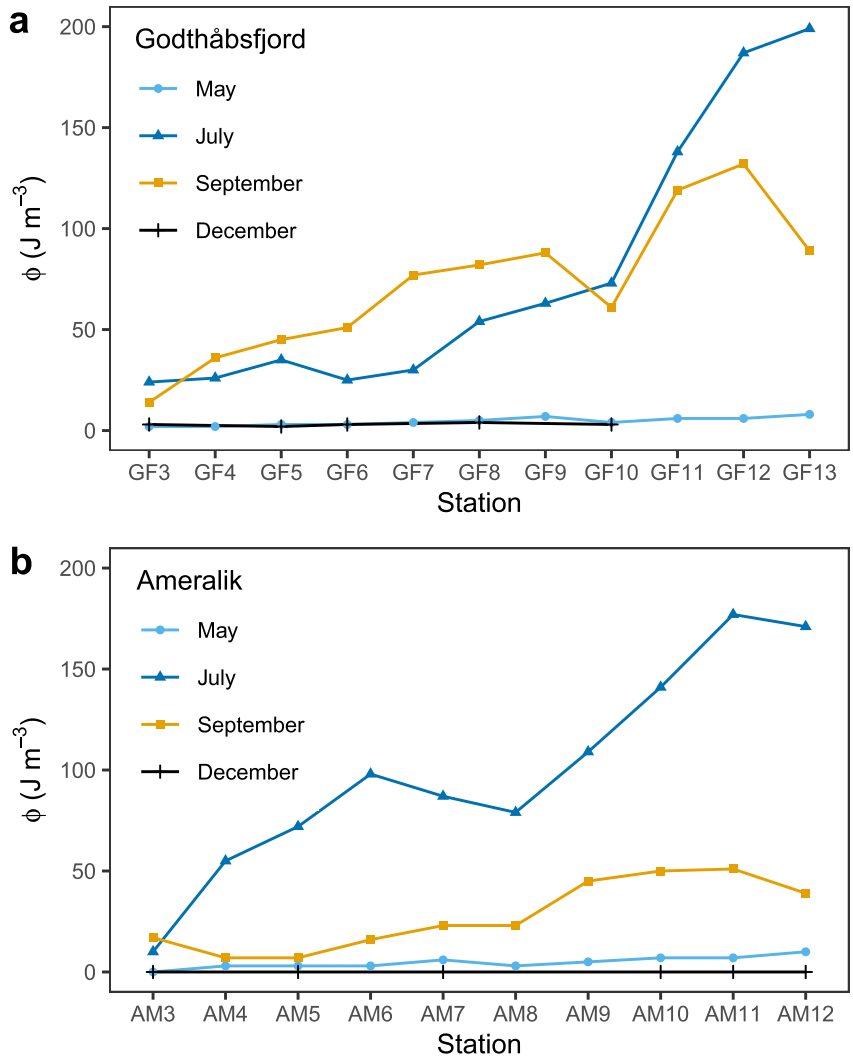

Figure 8. Stratification index (φ) for upper 50 m water depth layer of Ameralik (stations AM3 to AM12) and Godthåbsfjord (stations GF3 to GF13).

deepening of the isopycnals. In addition, mid-fjord (station AM5) potential density anomaly measurements show that there was greater change between May and December in intermediate depths (100 and 200 m, Figure 4c) than deeper in the water column (400 m, Figure 4d). The change in density from May to December observed at 400 m at AM5 (-0.024 kg m^{-3}) is indicative of diffusion processes and is an order of magnitude smaller than at 200 m (-0.325 kg m^{-3}) and 100 m (-0.514 kg m^{-3}) depths, indicating the existence of another exchange mechanism at 100 and 200 m depths. This supports our hypothesis, which is further evidenced by the finding made in Section 3.5 that sill region water was present in both outer and inner fjord stations of Ameralik and Godthåbsfjord. We hypothesise that, after forming in the outer sill region, this water mass was transported into the fjord by the intermediate baroclinic circulation, as has been verified in Godthåbsfjord through current measurements (Mortensen et al., 2014).

4.2. Impact of Sill Depth on Bottom Water Properties

A comparison of deep water properties reveals another important difference between these two fjords. Between 50 and 400 m, Ameralik was fresher (by 0.2) and cooler (by between 0.7 and 1.1°C) than Godthåbsfjord for each of the studied months (May, July and September). This difference also applied to the water below 400 m, as indicated by the gray rectangles in Figure 6. The difference in deep water properties is related to the sill depth,

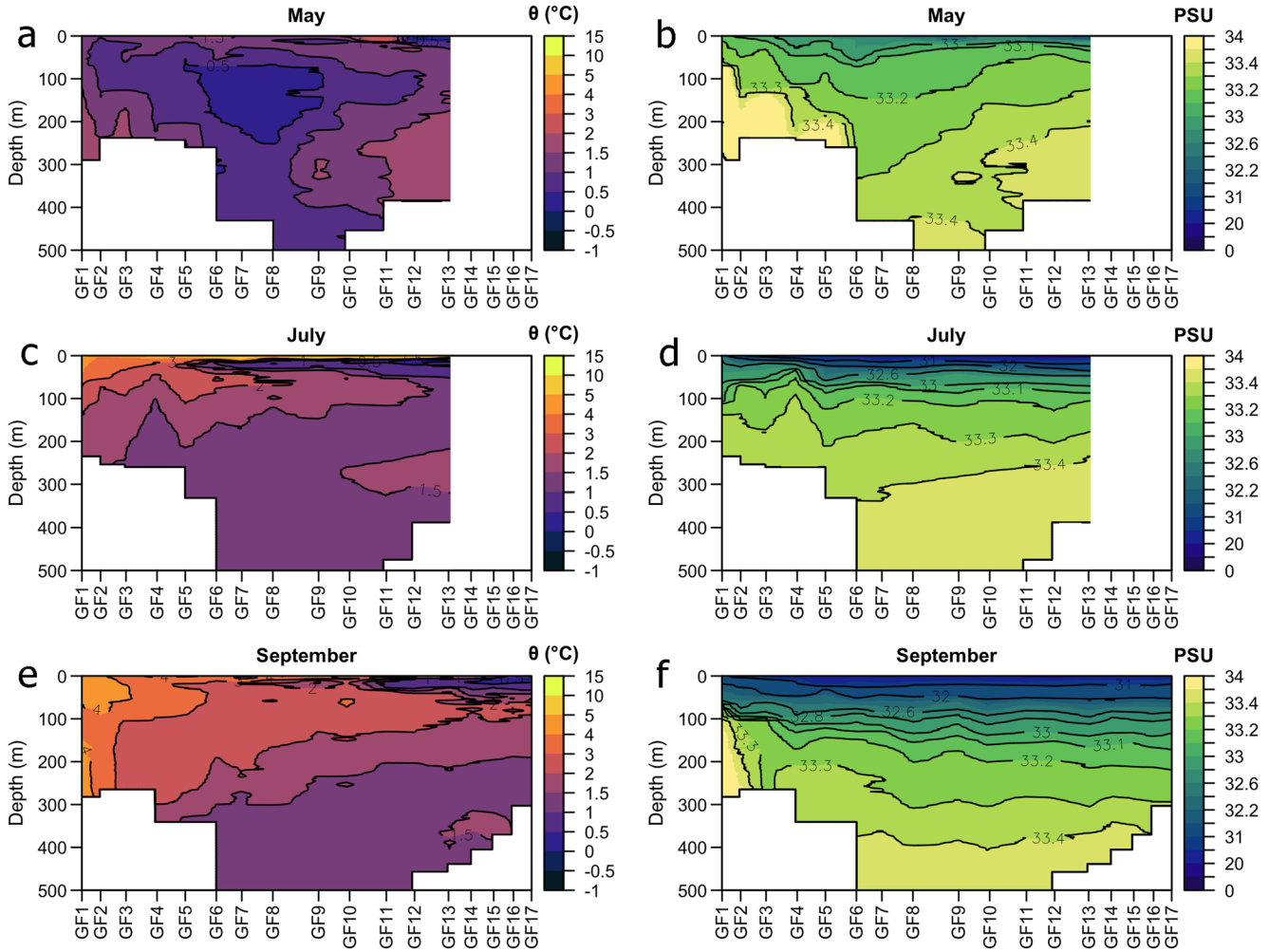

Figure 9. Potential temperature and practical salinity length sections of the upper 500 m of Godthåbsfjord in May, July and September 2019, from outer fjord (left) to inner fjord (right). Note that the length represented is greater in the September section, when favourable ice conditions allowed inner fjord stations GF14-17 to be sampled.

which determines the inflow of coastal water and differs between the two fjords. The entrance sill of Ameralik is ~110 m deep, compared to the ~200 m deep entrance sill of Godthåbsfjord. As a result, Ameralik receives less of the deeper, warmer and more saline subpolar mode water from the coastal region than Godthåbsfjord does. As this water makes its way into the fjord and mixes with local waters it eventually becomes part of the basin water. As such, the reduced inflow of subpolar mode water in Ameralik compared to Godthåbsfjord can explain the cooler and fresher deep water observed in Ameralik. This has important implications for the ecology due to distinct environmental preferences of species, as well as variation in the species transported in these different water masses (e.g., Grainger, 1963; Hirche, 1991; Hirche & Mumm, 1992).

4.3. Implication of Fjord Comparison

Comparing Ameralik with Godthåbsfjord demonstrates how the absence of marine-terminating glaciers, and thus of subglacial freshwater discharge, impacts the surface layer of the fjord (0–50 m), with Ameralik found to be more stratified on average than Godthåbsfjord in the summer (Figure 8). Increased summer stratification may be reflected in the future of fjords undergoing a retreat of glaciers onto land. This is in line with modeling predictions (e.g., Torsvik et al., 2019). The upwelling mechanism resulting from the subglacial discharge plumes has further implications for the nutrient distribution near the termini, which sustains primary production (Hopwood et al., 2018; Kanna et al., 2018; Meire et al., 2017) and extends support to the wider food web, including

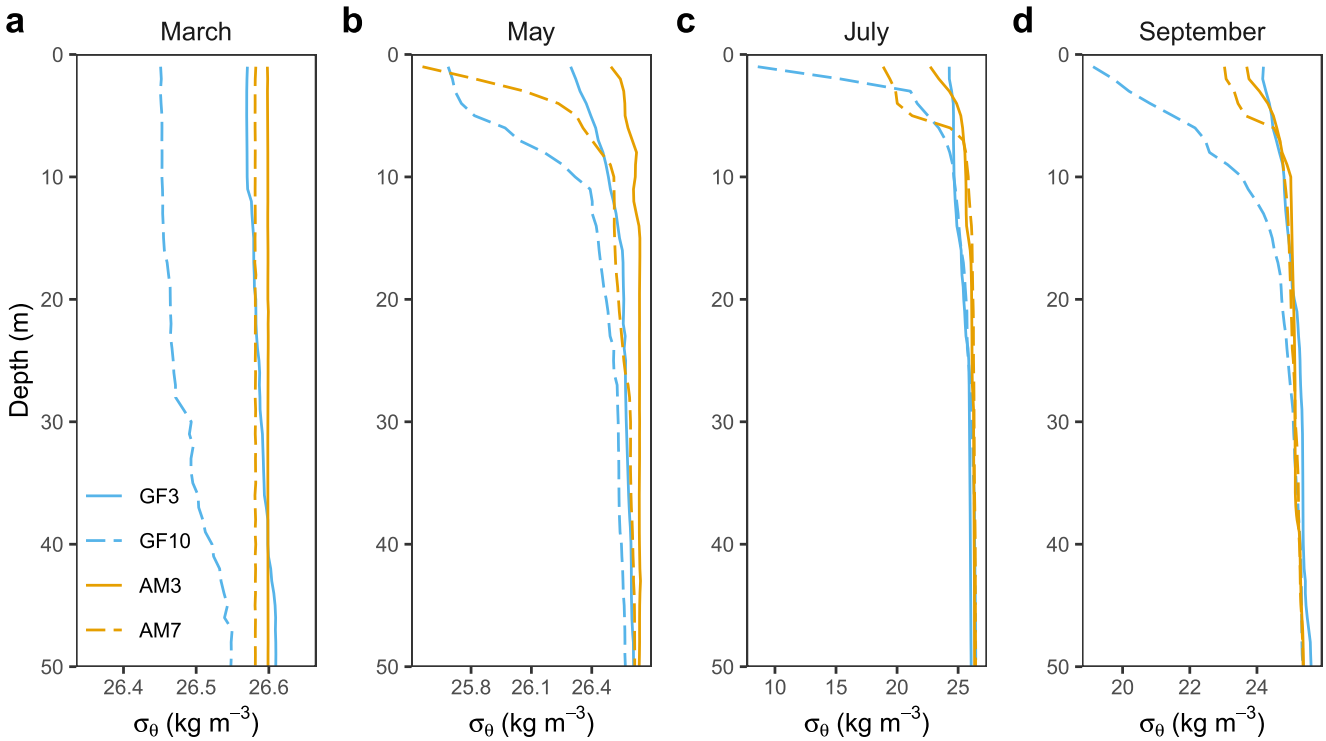

Figure 10. Potential density anomaly in upper 50 m water depth layer of Ameralik and Godthåbsfjord in (a) March, (b) May, (c) July, and (d) September 2019. Note that different scales are used for the *x*-axes.

marine mammals and seabirds (Lydersen et al., 2014; Urbanski et al., 2017). However, despite the higher summer stratification, the absence of a marine-terminating glacier does not necessarily mean a less dynamic fjord. We argue that there are three circulation modes in Ameralik, illustrated in Figures 11a and 11c. Dense coastal inflows across the sill during the winter of 2019–2020 had a major impact in the flushing of Ameralik through water renewal and induced internal upwelling. This prevented basin water from remaining stagnant through the whole year and contributed to the return of a weakly stratified state in winter. Meanwhile, the surface layer of Ameralik was modified through estuarine circulation (driven by freshwater from river runoff) and wind forcing. Tides are likely to have had an impact on mixing in Ameralik, with its location in the Davis Strait as one of the regions of Greenland's coast with the highest tidal ranges (Padman et al., 2018) and its shared entrance with Godthåbsfjord, which is highly turbulent (Mortensen et al., 2018). The tidal-induced mixing in the outer sill region most likely contributed to the setup of an intermediate baroclinic circulation, which resulted in the exchange of water at intermediate depths and consequently plays an important role in redistributing heat and freshwater in the fjord (Mortensen et al., 2014).

The circulation activity in fjords impacted only by land-terminating glaciers is set by boundary conditions including the sill depth, fjord geometry, coastal water masses, tidal currents, annual freshwater input (glacial water and net precipitation) and regional climatic conditions, all of which vary considerably across the fjords of Greenland. In contrast to the bottom water renewal observed in Ameralik, long term mooring data from the Young Sound/Tyrolerfjord system on the northeast coast of Greenland show that bottom water renewal did not occur in the period between 2004 and 2014 (Boone et al., 2018). The relatively shallow (~45 m) outer sill strongly restricts deep water renewal. Ongoing freshening in the coastal water in East Greenland further reduces the chance that it will exceed the density of the fjord basin water, which is necessary for coastal water to be able to reach these depths (Boone et al., 2018; Sejr et al., 2017).

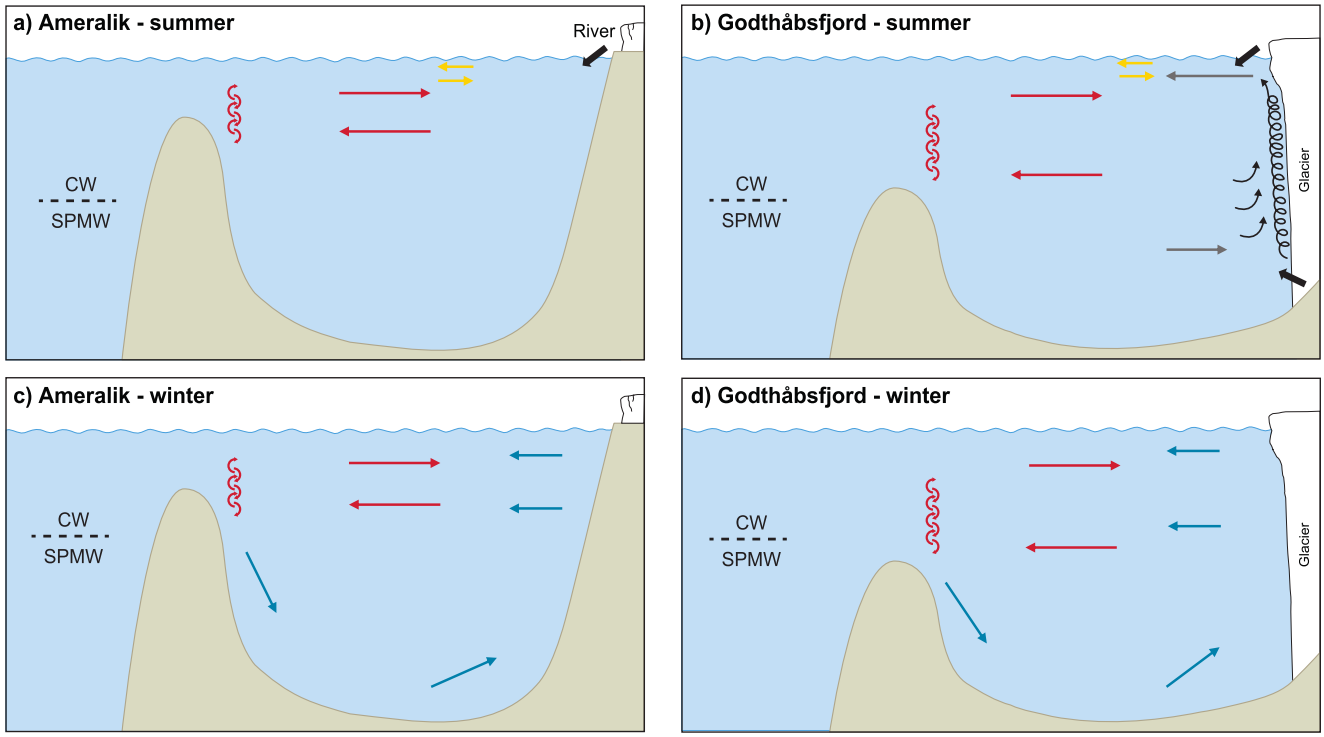

Figure 11. Conceptual diagrams of circulation modes and coastal water masses during summer and winter in Ameralik (a, c) and Godthåbsfjord (b, d). Thick black arrows represent freshwater input (surface runoff and subglacial meltwater discharge). Thin black arrows represent entrainment into the subglacial plume. Thin colored arrows represent net effects of circulation modes: yellow for estuarine circulation, red for intermediate baroclinic circulation, gray for subglacial circulation and blue for dense coastal inflows.

5. Summary and Conclusions

Ameralik, in southwest Greenland, represents the stage of a fjord after its glaciers have retreated from a marine-terminating to a land-terminating position. In this study we provide the first description of its hydrography, and compare our findings with the neighboring Godthåbsfjord, which is impacted by both land- and marine-terminating glaciers.

The absence of a marine-terminating glacier, and therefore of glacial ice and subglacial discharge, has implications for the hydrography and circulation. In 2019, spring and summer months in Ameralik were characterized by the transition from a weakly stratified fjord to a fresher, highly stratified fjord with a strong halocline and an estuarine circulation resulting from freshwater runoff. We found that a large fraction of the freshwater input is retained inside the fjord during the summer and autumn months, which we propose occurred through intermediate baroclinic circulation. During this period the upper 50 m water layer was considerably warmer in Ameralik than in Godthåbsfjord. Autumn and winter represented a steady return toward the pre-spring conditions, as freshwater runoff was strongly reduced, and export of summer accumulated freshwater from the fjord occurred, which we propose was related to coastal inflows. This resulted in flushing of the fjord and restored the system to a weakly stratified state. The shallower main sill of Ameralik with respect to that of Godthåbsfjord resulted in the intrusion of less of the subpolar mode water that is warmer and more saline compared to the overlying southwest Greenland coastal water. This produced differences in the fjord water properties which may be important for fjord ecology. Tides are likely to play a major role in mixing in the fjord, with tidal-induced mixing contributing to the setup of an intermediate baroclinic circulation in the fjord, as identified from the downward temporal movement of isopycnals at mid-depths and the inferred in-fjord transportation of sill region water in Ameralik. This case study demonstrates the importance of physical features, such as bathymetry and glacier type, as well as coastal water masses for the hydrography of Greenland fjords.

Data Availability Statement

Processed CTD, mooring and weather data are available at the World Data Center PANGAEA (Stuart-Lee et al., 2021a, 2021b, 2021c).

Acknowledgments
L. Meire was funded by research program VENI with project 016.Veni.192.150 from the Dutch Research Council (NWO). Meteorological data from Nuuk were provided by Asiaq Greenland Survey, Nuuk, Greenland. We would like to thank Flemming Heinrich and the crew of RV SANNA, Peter Rosvig Pedersen of the Polar Diver, Anders Pedersen and the crew of the Tulu for field assistance.

References

Abermann, J., Eckerstorfer, M., Malnes, E., & Hansen, B. U. (2019). A large wet snow avalanche cycle in West Greenland quantified using remote sensing and in situ observations. *Natural Hazards*, *97*(2), 517–534. https://doi.org/10.1007/s11069-019-03655-8

Arendt, K. E., Agersted, M. D., Sejr, M. K., & Juul-Pedersen, T. (2016). Glacial meltwater influences on plankton community structure and the importance of top-down control (of primary production) in a NE Greenland fjord. *Estuarine, Coastal and Shelf Science*, *183*, 123–135. https://doi.org/10.1016/j.ecss.2016.08.026

Beaird, N. L., Straneo, F., & Jenkins, W. (2018). Export of strongly diluted Greenland meltwater from a major glacial fjord. *Geophysical Research Letters*, *45*(9), 4163–4170. https://doi.org/10.1029/2018gl077000

Bendtsen, J., Mortensen, J., Lennert, K., & Rysgaard, S. (2015). Heat sources for glacial ice melt in a west Greenland tidewater outlet glacier fjord: The role of subglacial freshwater discharge. *Geophysical Research Letters*, *42*(10), 4089–4095. https://doi.org/10.1002/2015gl063846

Bendtsen, J., Mortensen, J., & Rysgaard, S. (2014). Seasonal surface layer dynamics and sensitivity to runoff in a high Arctic fjord (Young Sound/Tyrolerfjord, 74°N). *Journal of Geophysical Research: Oceans*, *119*(9), 6461–6478. https://doi.org/10.1002/2014JC010077

Boone, W., Rysgaard, S., Carlson, D. F., Meire, L., Kirillov, S., Mortensen, J., et al. (2018). Coastal freshening prevents fjord bottom water renewal in Northeast Greenland: A mooring study from 2003 to 2015. *Geophysical Research Letters*, *45*(6), 2726–2733. https://doi.org/10.1002/2017gl076591

Boone, W., Rysgaard, S., Kirillov, S., Dmitrenko, I., Bendtsen, J., Mortensen, J., et al. (2017). Circulation and fjord-shelf exchange during the ice-covered period in Young Sound-Tyrolerfjord, Northeast Greenland (74 N). *Estuarine, Coastal and Shelf Science*, *194*, 205–216. https://doi.org/10.1016/j.ecss.2017.06.021

Dmitrenko, I. A., Kirillov, S. A., Rysgaard, S., Barber, D. G., Babb, D. G., Pedersen, L. T., et al. (2015). Polynya impacts on water properties in a Northeast Greenland fjord. *Estuarine, Coastal and Shelf Science*, *153*, 10–17. https://doi.org/10.1016/j.ecss.2014.11.027

Grainger, E. H. (1963). Copepods of the genus Calanus as indicators of eastern Canadian waters. *Marine distributions*, 68–94. https://doi.org/10.3138/9781442654020-007

Hirche, H. J. (1991). Distribution of dominant calanoid copepod species in the Greenland Sea during late fall. *Polar Biology*, *11*(6), 351–362. https://doi.org/10.1007/bf00239687

Hirche, H. J., & Mumm, N. (1992). Distribution of dominant copepods in the Nansen Basin, Arctic Ocean, in summer. *Deep Sea Research Part A. Oceanographic Research Papers*, *39*(2), S485–S505. https://doi.org/10.1016/s0198-0149(06)80017-8

Hopwood, M. J., Carroll, D., Browning, T. J., Meire, L., Mortensen, J., et al. (2018). Non-linear response of summertime marine productivity to increased meltwater discharge around Greenland. *Nature Communications*, *9*(1), 1–9. https://doi.org/10.1038/s41467-018-05488-8

Kanna, N., Sugiyama, S., Ohashi, Y., Sakakibara, D., Fukamachi, Y., & Nomura, D. (2018). Upwelling of macronutrients and dissolved inorganic carbon by a subglacial freshwater driven plume in Bowdoin Fjord, northwestern Greenland. *Journal of Geophysical Research: Biogeosciences*, *123*(5), 1666–1682. https://doi.org/10.1029/2017jg004248

King, M. D., Howat, I. M., Candela, S. G., Noh, M. J., Jeong, S., Noël, B. P., et al. (2020). Dynamic ice loss from the Greenland Ice Sheet driven by sustained glacier retreat. *Communications Earth & Environment*, *1*(1), 1–7. https://doi.org/10.1038/s43247-020-0001-2

Langen, P. L., Mottram, R. H., Christensen, J. H., Boberg, F., Rodehacke, C. B., Stendel, M., et al. (2015). Quantifying energy and mass fluxes controlling Godthåbsfjord freshwater input in a 5-km simulation (1991–2012). *Journal of Climate*, *28*(9), 3694–3713. https://doi.org/10.1175/jcli-d-14-00271.1

Lin, P., Pickart, R. S., Torres, D. J., & Pacini, A. (2018). Evolution of the freshwater coastal current at the southern tip of Greenland. *Journal of Physical Oceanography*, *48*(9), 2127–2140. https://doi.org/10.1175/jpo-d-18-0035.1

Lund-Hansen, L. C., Hawes, I., Holtegaard Nielsen, M., Dahllöf, I., & Sorrell, B. K. (2018). Summer meltwater and spring sea ice primary production, light climate and nutrients in an Arctic estuary, Kangerlussuaq, west Greenland. *Arctic Antarctic and Alpine Research*, *50*(1), S100025. https://doi.org/10.1080/15230430.2017.1414468

Lydersen, C., Assmy, P., Falk-Petersen, S., Kohler, J., Kovacs, K. M., Reigstad, M., et al. (2014). The importance of tidewater glaciers for marine mammals and seabirds in Svalbard, Norway. *Journal of Marine Systems*, *129*, 452–471. https://doi.org/10.1016/j.jmarsys.2013.09.006

MacKenzie, L., & Adamson, J. (2004). Water column stratification and the spatial and temporal distribution of phytoplankton biomass in Tasman Bay, New Zealand: Implications for aquaculture. *New Zealand Journal of Marine and Freshwater Research*, *38*(4), 705–728. https://doi.org/10.1080/00288330.2004.9517271

Mankoff, K. D., Straneo, F., Cenedese, C., Das, S. B., Richards, C. G., & Singh, H. (2016). Structure and dynamics of a subglacial discharge plume in a Greenlandic fjord. *Journal of Geophysical Research: Oceans*, *121*(12), 8670–8688. https://doi.org/10.1002/2016jc011764

Meire, L., Mortensen, J., Meire, P., Juul-Pedersen, T., Sejr, M. K., Rysgaard, S., et al. (2017). Marine-terminating glaciers sustain high productivity in Greenland fjords. *Global Change Biology*, *23*(12), 5344–5357. https://doi.org/10.1111/gcb.13801

Meire, L., Søgaard, D. H., Mortensen, J., Meysman, F. J. R., Soetaert, K., Arendt, K. E., et al. (2015). Glacial meltwater and primary production are drivers of strong CO_2 uptake in fjord and coastal waters adjacent to the Greenland Ice Sheet. *Biogeosciences*, *12*(8), 2347–2363. https://doi.org/10.5194/bg-12-2347-2015

Monteban, D., Pedersen, J. O. P., & Nielsen, M. H. (2020). Physical oceanographic conditions and a sensitivity study on meltwater runoff in a West Greenland fjord: Kangerlussuaq. *Oceanologia*, *62*(4), 460–477. https://doi.org/10.1016/j.oceano.2020.06.001

Mortensen, J., Bendtsen, J., Lennert, K., & Rysgaard, S. (2014). Seasonal variability of the circulation system in a west Greenland tidewater outlet glacier fjord, Godthåbsfjord (64°N): Godthåbsfjord. *Journal of Geophysical Research: Earth Surface*, *119*(12), 2591–2603. https://doi.org/10.1002/2014JF003267

Mortensen, J., Bendtsen, J., Motyka, R. J., Lennert, K., Truffer, M., Fahnestock, M., et al. (2013). On the seasonal freshwater stratification in the proximity of fast-flowing tidewater outlet glaciers in a sub-Arctic sill fjord: Godthåbsfjord. *Journal of Geophysical Research: Oceans*, *118*(3), 1382–1395. https://doi.org/10.1002/jgrc.20134

Mortensen, J., Lennert, K., Bendtsen, J., & Rysgaard, S. (2011). Heat sources for glacial melt in a sub-Arctic fjord (Godthåbsfjord) in contact with the Greenland Ice Sheet. *Journal of Geophysical Research*, *116*(C1), C01013. https://doi.org/10.1029/2010JC006528

Mortensen, J., Rysgaard, S., Arendt, K. E., Juul-Pedersen, T., Søgaard, D. H., Bendtsen, J., et al. (2018). Local coastal water masses control heat levels in a West Greenland tidewater outlet glacier fjord. *Journal of Geophysical Research: Oceans*, *123*(11), 8068–8083. https://doi.org/10.1029/2018jc014549

Mortensen, J., Rysgaard, S., Bendtsen, J., Lennert, K., Kanzow, T., Lund, H., et al. (2020). Subglacial discharge and its Down-Fjord transformation in West Greenland Fjords with an ice mélange. *Journal of Geophysical Research Oceans*, *125*(9). https://doi.org/10.1029/2020JC016301

Mouginot, J., Rignot, E., Bjørk, A. A., Van den Broeke, M., Millan, R., Morlighem, M., et al. (2019). Forty-six years of Greenland Ice Sheet mass balance from 1972 to 2018. *Proceedings of the National Academy of Sciences*, *116*(19), 9239–9244. https://doi.org/10.1073/pnas.1904242116

Nielsen, M. H., Erbs-Hansen, D. R., & Luise, K. (2010). Water masses in Kangerlussuaq, a large fjord in West Greenland: The processes of formation and the associated foraminiferal fauna. *Polar Research*, *29*(2), 159–175. https://doi.org/10.1111/j.1751-8369.2010.00147.x

Overeem, I., Hudson, B., Welty, E., Mikkelsen, A., Bamber, J., Petersen, D., et al. (2015). River inundation suggests ice-sheet runoff retention. *Journal of Glaciology*, *61*(228), 776–788. https://doi.org/10.3189/2015JoG15J012

Padman, L., Siegfried, M. R., & Fricker, H. A. (2018). Ocean tide influences on the Antarctic and Greenland ice sheets. *Reviews of Geophysics*, *56*(1), 142–184. https://doi.org/10.1002/2016rg000546

R Core Team. (2013). *R: A language and environment for statistical computing*. R Development Core Team.

Richter, A., Rysgaard, S., Dietrich, R., Mortensen, J., & Petersen, D. (2011). Coastal tides in West Greenland derived from tide gauge records. *Ocean Dynamics*, *61*(1), 39–49. https://doi.org/10.1007/s10236-010-0341-z

Rignot, E., Xu, Y., Menemenlis, D., Mouginot, J., Scheuchl, B., Li, X., et al. (2016). Modeling of ocean-induced ice melt rates of five west Greenland glaciers over the past two decades. *Geophysical Research Letters*, *43*(12), 6374–6382. https://doi.org/10.1002/2016GL068784

Rysgaard, S., Boone, W., Carlson, D., Sejr, M. K., Bendtsen, J., Juul-Pedersen, T., et al. (2020). An updated view on water masses on the pan-West Greenland Continental Shelf and their link to proglacial Fjords. *Journal of Geophysical Research: Oceans*, *125*(2). https://doi.org/10.1029/2019JC015564

Rysgaard, S., Vang, T., Stjernholm, M., Rasmussen, B., Windelin, A., & Kiilsholm, S. (2003). Physical conditions, carbon transport, and climate change impacts in a Northeast Greenland Fjord. *Arctic, Antarctic, and Alpine Research*, *35*(3), 301–312. https://doi.org/10.1657/1523-0430(2003)035[0301:pcctac]2.0.co;2

Sciascia, R., Straneo, F., Cenedese, C., & Heimbach, P. (2013). Seasonal variability of submarine melt rate and circulation in an East Greenland fjord. *Journal of Geophysical Research: Oceans*, *118*(5), 2492–2506. https://doi.org/10.1002/jgrc.20142

Sejr, M. K., Stedmon, C. A., Bendtsen, J., Abermann, J., Juul-Pedersen, T., Mortensen, J., et al. (2017). Evidence of local and regional freshening of Northeast Greenland coastal waters. *Scientific Reports*, *7*(1), 1–6. https://doi.org/10.1038/s41598-017-10610-9

Shepherd, A., Ivins, E., Rignot, E., Smith, B., van den Broeke, M., Velicogna, I., et al. (2020). Mass balance of the Greenland Ice Sheet from 1992 to 2018. *Nature*, *579*(7798), 233–239. https://doi.org/10.1038/s41586-019-1855-2

Simonsen, S. B., Barletta, V. R., Colgan, W. T., & Sørensen, L. S. (2021). Greenland Ice Sheet Mass Balance (1992–2020) From Calibrated Radar Altimetry. *Geophysical Research Letters*, *48*(3). https://doi.org/10.1029/2020GL091216

Simpson, J. H. (1981). The shelf-sea fronts: Implications of their existence and behaviour. *Philosophical Transactions of the Royal Society of London - Series A: Mathematical and Physical Sciences*, *302*(1472), 531–546. https://doi.org/10.1098/rsta.1981.0181

Smith, B., Fricker, H. A., Gardner, A. S., Medley, B., Nilsson, J., Paolo, F. S., et al. (2020). Pervasive ice sheet mass loss reflects competing ocean and atmosphere processes. *Science*, *368*(6496), 1239–1242. https://doi.org/10.1126/science.aaz5845

Straneo, F., & Cenedese, C. (2015). The Dynamics of Greenland's Glacial Fjords and their role in climate. *Annual Review of Marine Science*, *7*(1), 89–112. https://doi.org/10.1146/annurev-marine-010213-135133

Straneo, F., Curry, R. G., Sutherland, D. A., Hamilton, G. S., Cenedese, C., Våge, K., et al. (2011). Impact of Fjord dynamics and glacial runoff on the circulation near Helheim Glacier. *Nature Geoscience*, *4*(5), 322–327. https://doi.org/10.1038/ngeo1109

Stuart-Lee, A., Meire, L., & Mortensen, J. (2021a). *Seasonal temperature and salinity depth measurements from southwest Greenland fjords in 2019*. PANGAEA. https://doi.org/10.1594/PANGAEA.933610

Stuart-Lee, A., Meire, L., & Mortensen, J. (2021b). *Seasonal temperature and salinity measurements from a mooring in Ameralik fjord in 2019*. PANGAEA. https://doi.org/10.1594/PANGAEA.933706

Stuart-Lee, A., Meire, L., & Mortensen, J. (2021c). *Weather data from a southwest Greenland fjord, Ameralik, in 2019*. PANGAEA. https://doi.org/10.1594/PANGAEA.933635

Svendsen, H., Beszczynska-Møller, A., Hagen, J. O., Lefauconnier, B., Tverberg, V., Gerland, S., et al. (2002). The physical environment of Kongsfjorden–Krossfjorden, an Arctic fjord system in Svalbard. *Polar Research*, *21*(1), 133–166. https://doi.org/10.1111/j.1751-8369.2002.tb00072.x

Torsvik, T., Albretsen, J., Sundfjord, A., Kohler, J., Sandvik, A. D., Skarðhamar, J., et al. (2019). Impact of tidewater glacier retreat on the fjord system: Modeling present and future circulation in Kongsfjorden, Svalbard. *Estuarine, Coastal and Shelf Science*, *220*, 152–165. https://doi.org/10.1016/j.ecss.2019.02.005

Urbanski, J. A., Stempniewicz, L., Węsławski, J. M., Dragańska-Deja, K., Wochna, A., Goc, M., et al. (2017). Subglacial discharges create fluctuating foraging hotspots for sea birds in tidewater glacier bays. *Scientific Reports*, *7*(1), 1–12. https://doi.org/10.1038/srep43999

Van As, D., Andersen, M. L., Petersen, D., Fettweis, X., Van Angelen, J. H., Lenaerts, J. T., et al. (2014). Increasing meltwater discharge from the Nuuk region of the Greenland ice sheet and implications for mass balance (1960–2012). *Journal of Glaciology*, *60*(220), 314–322. https://doi.org/10.3189/2014jog13j065